Quantum state transfer using stimulated Raman adiabatic passage under a dissipative environment

Q. Z. Hou,[1] W. L. Yang,[2,*] M. Feng,[1,2,†] and C.-Y. Chen[1,3,‡]

[1]*Department of Physics and Key Laboratory of Low-Dimensional Quantum Structures and Quantum Control of Ministry of Education, Hunan Normal University, Changsha 410081, China*

[2]*State Key Laboratory of Magnetic Resonance and Atomic and Molecular Physics, Wuhan Institute of Physics and Mathematics, Chinese Academy of Sciences, Wuhan 430071, China*

[3]*Department of Physics and Information Engineering, Hunan Institute of Humanities, Science and Technology, Loudi 417000, China*

(Received 3 April 2013; published 8 July 2013)

We propose a potentially practical scheme to realize arbitrary quantum state transfer between two traveling atoms that go through a high-finesse cavity by using stimulated Raman adiabatic passage in an atom-cavity-laser system under a dissipative environment. By numerically simulating the dynamics of the system, we demonstrate quantitatively that the fidelities of the quantum state transferred between two atoms can be maximized by elaborately adjusting the peak amplitudes of the laser's Rabi frequency and the detuning of the Raman transition. Additionally, the noise effect from the atomic and cavity dissipation can reduce the fidelity. The experimental feasibility is justified using currently available technology.

DOI: 10.1103/PhysRevA.88.013807 PACS number(s): 42.50.Pq, 32.80.Qk, 42.50.Ex, 03.65.Yz

I. INTRODUCTION

Recently, the adiabatic passage technique [1–4] developed in the adiabatic theorem has shown fruitful application in quantum state control and quantum information processing (QIP) such as coherent population trapping [5], lasing without population inversion [6], and nonclassical state engineering [7]. It is well known that adiabatic passage techniques mainly include the stimulated Raman adiabatic passage (STIRAP) [1,8–12], adiabatic rapid passage [13–16], Raman chirped adiabatic passage [17–19], Stark chirped rapid adiabatic passage [20–22], piecewise adiabatic passage [23,24], and bichromatic adiabatic passage [25].

These adiabatic passage techniques possess significant advantages such as robustness to environmental noises and parametric fluctuation. However, the dynamics regarding the adiabatic passage techniques was not studied sufficiently in dissipative systems. It is widely believed that the unavoidable interaction with the environment results in the system being in decoherence and also in other novel phenomena, thereby the dissipation plays an increasingly critical role in the field of QIP. As a result, it is instructive and interesting to investigate more rigorously the above-mentioned adiabatic passage process by explicitly considering the coupling between the system and the external environment [26].

In the present work, we focus on an atom-cavity system using the STIRAP technique in a dissipative environment, where a pair of Λ-type atoms pass through the cavity along opposite directions with each atom interacting nearly resonantly with the cavity mode and the laser pulse. In our model, the noise effects from the atomic spontaneous emission and the cavity dissipation are treated phenomenologically by the Markovian master equation in Lindblad form. Based on this model, we show the possibility of realizing arbitrary quantum state transfer (QST) between the two traveling atoms in a STIRAP process by elaborately adjusting the atom-cavity and atom-laser coupling strengths and the detuning in the Raman transition, where the peak amplitudes of the Rabi frequencies should satisfy the condition $G_0 \gg \Omega_0$ with G_0 (Ω_0) the peak amplitudes of Rabi frequencies of the atom-cavity (atom-laser) coupling. The relationship between the fidelities and the peak amplitudes of the laser's Rabi frequency in the dissipative and nondissipative cases are numerically analyzed through transforming the Markovian master equation from the Lindblad form to the Redfield form. We also show that the STIRAP process can be optimized by elaborately adjusting the values of detuning and the presence of a dissipative environment reduces the fidelity of the quantum state transferred.

The remainder of this paper is organized as follows. We describe the model of our system in Sec. II by introducing the Lindblad master equation for the noise effect. In Sec. III we implement the QST between two traveling atoms using the STIRAP technique and investigate the quantitative relation between the fidelities and the peak amplitude of the laser's pulse and the detuning, respectively. We discuss our results in Sec. IV and summarize in Sec. V.

II. SYSTEM AND MODEL

As illustrated in Fig. 1(a), the atom-cavity-laser system under consideration consists of two atoms passing through a high-finesse cavity with the same velocity v in opposite directions along the z axis. Additionally, the transmission of the laser beam is parallel to the y axis (i.e., perpendicular to the page). Each of the atoms consists of three levels and interacts with the cavity mode and a laser by a Λ-type structure, as shown in Fig. 1(b), where the cavity mode with the frequency ω_c is in near resonance with the transition $|e\rangle \Leftrightarrow |f\rangle$ (with the frequency ω_{ef}) and a laser beam with the frequency ω_L couples to the transition $|e\rangle \Leftrightarrow |g\rangle$ (with the frequency ω_{eg}).

Without loss of generality, we consider the Rabi frequencies $\Omega_j(t)$ and $G_j(t)$ to be real and positive and denote the detunings of the laser and cavity fields from the atomic transition frequencies by $\Delta = \omega_{eg} - \omega_L = \omega_{ef} - \omega_c$, where for simplicity we assume $\omega_{eg1} = \omega_{eg2} = \omega_{eg}$ and

*ywl@wipm.ac.cn
†mangfeng@wipm.ac.cn
‡chenchangyong_64@hotmail.com

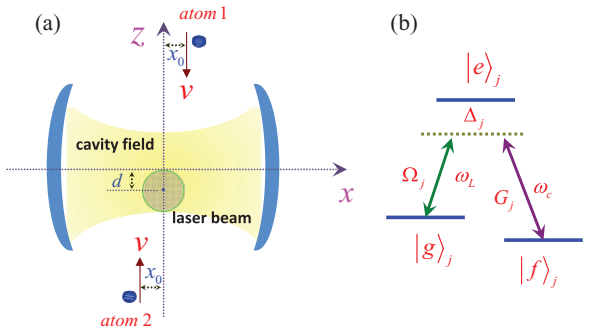

FIG. 1. (Color online) (a) Schematic setup for the STIRAP process in the atom-cavity-laser system, where two atoms pass through the cavity and couple to the laser beam propagating along the y axis (perpendicular to the page). (b) Level structure of the atoms with two nondegenerate ground states $|g\rangle_j$ and $|f\rangle_j$ and an excited state $|e\rangle_j$, where the subscript j ($j = 1,2$) denotes the two atoms. Here Δ_j is the detuning and $\Omega_j(t)$ and $G_j(t)$ are the atom-laser and atom-cavity coupling strengths, respectively.

$\omega_{ef1} = \omega_{ef2} = \omega_{ef}$. Controlled by the STIRAP process, the time-dependent atom-cavity coupling strengths and the delayed Rabi frequencies of the laser encountered by the traveling atoms can be written as

$$G_1(t) = G_0 \exp\left[-\left(\frac{vt + d/m}{W_C}\right)^2\right] \cos\left(\frac{2\pi x_0}{\lambda}\right), \quad (1)$$

$$G_2(t) = G_0 \exp\left[-\left(\frac{vt + d/n}{W_C}\right)^2\right] \cos\left(\frac{-2\pi x_0}{\lambda}\right), \quad (2)$$

$$\Omega_1(t) = \Omega_0 \exp\left[-\left(\frac{vt + d/p}{W_L}\right)^2\right] e^{-x_0^2/W_L^2}, \quad (3)$$

$$\Omega_2(t) = \Omega_0 \exp\left[-\left(\frac{vt + d/q}{W_L}\right)^2\right] e^{-x_0^2/W_L^2}, \quad (4)$$

where λ is the wavelength of the transition $|e\rangle \Leftrightarrow |f\rangle$; d is the distance from the cavity center to the center of the laser beam; m, n, p, and q are random constants, which meet the condition that $m^{-1} - p^{-1} = 1$ and $q^{-1} - n^{-1} = 1$; and W_C and W_L are the waists of the cavity and the laser beam, respectively. In addition, $G_0 = -\mu\sqrt{\omega_C/2\epsilon_0 V}$ and $\Omega_0 = -\mu\epsilon_L$ ($G_0, \Omega_0 \ll \omega_{eg}, \omega_{ef}$) are the peak amplitudes of the atom-cavity coupling and the laser's Rabi frequency, where μ, V, ϵ_0, and ϵ_L are the atomic dipole moment, the effective volume of the cavity mode, the free-space permittivity, and the amplitude of the laser field, respectively.

Under the rotating-wave approximation, we have the Hamiltonian of system in the interaction picture in units of $\hbar = 1$,

$$H(t) = \sum_{j=1,2} \{\Delta_j |e\rangle_{jj}\langle e| + [G_j(t)a|e\rangle_{jj}\langle f| + \text{H.c.}] + [\Omega_j(t)|e\rangle_{jj}\langle g| + \text{H.c.}]\} + \delta a^\dagger a, \quad (5)$$

where a ($a^\dagger$) is the annihilation (creation) operator of the cavity mode and $\delta = \omega_C - \omega_L$ is taken to be positive and much smaller than the values of ω_C and ω_L. We take into account the noise effects from the cavity dissipation and atomic spontaneous emission in this open system by phenomenologically exploiting the Markovian master equation in Lindblad form

$$\frac{d\rho}{dt} = -i[H(t), \rho] + \Gamma(\rho), \quad (6)$$

with

$$\Gamma(\rho) = \sum_{j=1}^{2} \left[\Gamma_{eg}\left(2\sigma_{ge}^j \rho \sigma_{eg}^j - \sigma_{eg}^j \sigma_{ge}^j \rho - \rho \sigma_{eg}^j \sigma_{ge}^j\right) + \Gamma_{ef}\left(2\sigma_{fe}^j \rho \sigma_{ef}^j - \sigma_{ef}^j \sigma_{fe}^j \rho - \rho \sigma_{ef}^j \sigma_{fe}^j\right)\right] + \kappa(2a\rho a^\dagger - a^\dagger a\rho - \rho a^\dagger a), \quad (7)$$

where $\Gamma_{eg(f)}$ is the radiative rate between $|e\rangle$ and $|g\rangle$ ($|f\rangle$), κ is the decay rate of the cavity, and $\sigma_{ge}^j = |g\rangle_{jj}\langle e|$, $\sigma_{eg}^j = |e\rangle_{jj}\langle g|$, $\sigma_{fe}^j = |f\rangle_{jj}\langle e|$, and $\sigma_{ef}^j = |e\rangle_{jj}\langle f|$. Thus the total decay rate of the excited state $|e\rangle$ is $\Gamma = \Gamma_{eg} + \Gamma_{ef}$ for each atom. In our case, the strong coupling regime with $G_0 \gg \Gamma, \kappa$ is required for realizing QST with high fidelities in the dissipative case. To simplify our calculation, we may transfer Eq. (6) from the Lindblad form to the Redfield form by the usual methods [27,28], which may yield a simpler numerical computation by changing the matrix differential equations to the vector differential equations (see details of our calculations in the Appendix).

III. QUANTUM STATE TRANSFER BETWEEN TWO ATOMS

It is an important task in the field of QIP to carry out efficient control of population transfer and QST [29]. In this section we explicitly describe the realization of arbitrary QST between the two moving atoms using the STIRAP process.

Suppose that at an initial time, the first atom in the cavity is prepared in an arbitrary superposition state $\alpha|g\rangle_1 + \beta|f\rangle_1$, but the second atom is in the state $|g\rangle_2$. Additionally, we assume that the cavity is initially prepared in the vacuum state $|0\rangle_c$. The goal in this scheme is to accomplish the following operation:

$$\begin{aligned} |\Psi_i(0)\rangle &= (\alpha|g\rangle_1 + \beta|f\rangle_1)|g\rangle_2|0\rangle_c \\ &\Downarrow \\ |\Psi_f(t)\rangle &= |g\rangle_1(\alpha|g\rangle_2 + \beta|f\rangle_2)|0\rangle_c, \end{aligned} \quad (8)$$

where the coefficients α and β satisfy the normalization condition $|\alpha|^2 + |\beta|^2 = 1$.

To simplify the numerical simulation, we transfer the master equation (6) into the Redfield form, which turns the calculation from the matrix equations to the vector differential equations (see the Appendix for details). In our case, the Hilbert space is spanned in $9(N + 1)$ dimensions with the density matrix elements of the form $\rho_{ij,mn,kl}$, where i, j, m, and n can be any of g, e, and f and i,m and j,n denote the states of atom 1 and atom 2, respectively. Here k and l represent the number of photons in the cavity with $k,l = 0,1,\ldots,N$.

Figure 2(a) shows the Rabi frequencies $G_j(t)$ and $\Omega_j(t)$ employed for QST, where the first atom enters the cavity before the second one in the experiment. To keep the cavity nearly all inside the vacuum state during the STIRAP process, the values of the Rabi frequency $\Omega_j(t)$ are taken to be much smaller

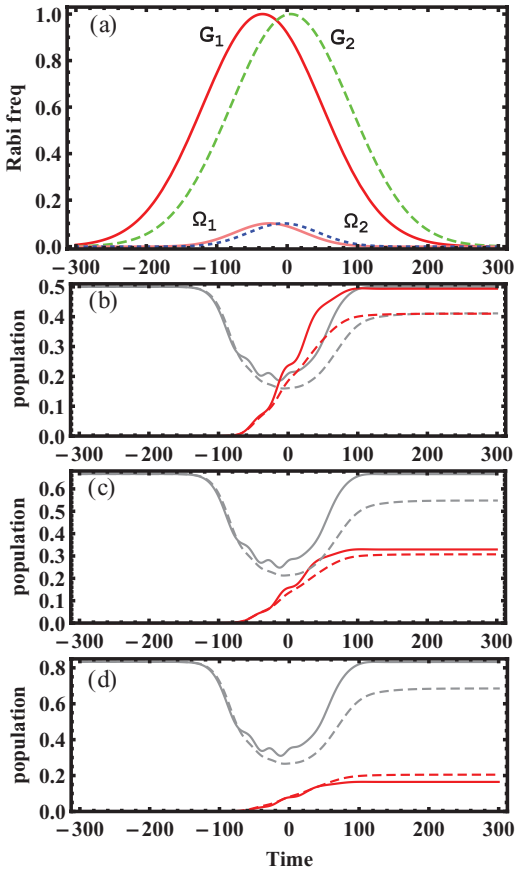

FIG. 2. (Color online) (a) Time evolution of Rabi frequencies $G_j(t)$ and $\Omega_j(t)$ for QST. The parameters are $G_0 = 1$, $\delta = 20G_0$, $\Delta_1 = \Delta_2 = \Delta = 0.1G_0$, $\Omega_0 = 0.1G_0$, $W_C = 120v/G_0$, $W_L = 70v/G_0$, $d = 10v/G_0$, $x_0 = \lambda$, and the random constants $m = 2/7$, $n = -2$, $p = 2/5$, and $q = 2$. Also shown is the time-dependent population of the target state in QST during the STIRAP process from different initial states: (b) $\alpha = \sqrt{1/2}$, $\beta = \sqrt{1/2}$; (c) $\alpha = \sqrt{2/3}$, $\beta = \sqrt{1/3}$; and (d) $\alpha = \sqrt{5/6}$, $\beta = \sqrt{1/6}$. The gray solid and red solid lines represent the populations of the states $|g\rangle_1|g\rangle_2|0\rangle_c$ and $|g\rangle_1|f\rangle_2|0\rangle_c$, respectively, in the nondissipative case of $\Gamma = \kappa = 0$. The gray dashed and red dashed lines represent the populations of the states $|g\rangle_1|g\rangle_2|0\rangle_c$ and $|g\rangle_1|f\rangle_2|0\rangle_c$, respectively, in the dissipative case of $\Gamma = G_0/30, \kappa = G_0/120$. The time parameter is dimensionless.

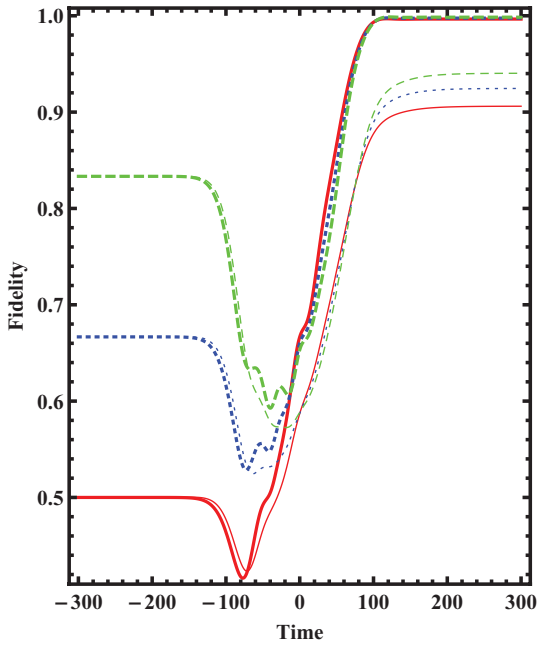

FIG. 3. (Color online) Time evolution of the fidelity of the target states $|\Psi_f\rangle$ in the case of $\Delta = 0.1G_0$, where the thick solid, thick dotted, and thick dashed lines represent the nondissipative case $\Gamma = \kappa = 0$. The thin solid, thin dotted, and thin dashed lines represent the dissipative case $\Gamma = G_0/30$, $\kappa = G_0/120$. The red solid, blue dotted, and green dashed lines represent the three different initial states with the parameters $\alpha = \sqrt{1/2}$ ($\beta = \sqrt{1/2}$), $\alpha = \sqrt{2/3}$ ($\beta = \sqrt{1/3}$), and $\alpha = \sqrt{5/6}$ ($\beta = \sqrt{1/6}$), respectively. The parameter $G_0 = 1$ is used and the time parameter is dimensionless.

than that of the Rabi frequency $G_j(t)$. Meanwhile, assuming Gaussian pulse profiles for $\Omega_j(t)$ and $G_j(t)$ of widths $T_L = W_L/v$ and $T_C = W_C/v$, respectively, we have the sufficient condition of this STIRAP process: $\Omega_0 T_L \gg 1$ and $G_0 T_C \gg 1$.

Figures 2(b)–2(d) present the time-dependent population of the two components $|g\rangle_1|g\rangle_2|0\rangle_c$ and $|g\rangle_1|f\rangle_2|0\rangle_c$ in the target state $|\Psi_f(t)\rangle$ in Eq. (8) from different initial states $|\Psi_i(0)\rangle$. As shown in Figs. 2(b)–2(d), the dynamical behavior of the populations is similar between the nondissipative case and dissipative case. The biggest difference is slight slow oscillation behavior displayed in the nondissipative case [the middle section of Figs. 2(b)–2(d)], which disappears when we take dissipation effect explicitly into account. The physical mechanism leading to this result is that this oscillation results from the complicated dynamics, which is controlled by the time-dependent relative phases in the Rabi frequencies of the cavity mode and laser field, as shown in Eqs. (1)–(4), where the time-dependent relative phases are actually tuned by the relative velocity or position of the two atoms. Additionally, the population of $|g\rangle_1|f\rangle_2|0\rangle_c$ in the dissipative case gradually exceeds that of the nondissipative case with an increase of the coefficient α.

Furthermore, the QST process can be characterized by the fidelity of the final state according to the expression $F = \langle\Psi_f|\rho(t)|\Psi_f\rangle$, where $|\Psi_f\rangle$ is the desired target state in Eq. (8) and $\rho(t)$ is the actual density matrix of the system at time t. As shown in Fig. 3, the fidelities F are described by these stepwise curves. In the nondissipative case, the corresponding thick curves show that the fidelity can be very close to 1 in the long-time limit and does not depend intensively on the initial states $|\Psi_i(0)\rangle$. By comparing the thick curves with the thin curves in Fig. 3, we find that the system-environment interaction is unfavorable for the fidelity of the QST. So to carry out our scheme efficiently and with high fidelity, we have to suppress these noise effect as much as we can.

Being an adiabatic technique, the STIRAP process reaches an efficiency of unity only in the adiabatic limit and is insensitive to small or even moderate variations of most experimental parameters such as the pulse widths, pulse delay, pulse amplitudes, and single-photon detuning. Figure 4(a) shows the dependence of the fidelities on the peak amplitudes of the laser's Rabi frequency during the STIRAP process in the long-time limit. Note that the relationship between the fidelities and the coupling strength can be described

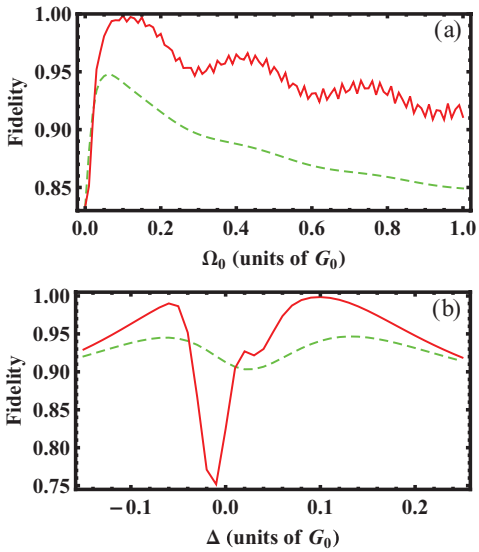

FIG. 4. (Color online) Dependence of the fidelity on the peak amplitudes of (a) the Rabi frequency and (b) the detunings in the long-time limit, where $G_0 = 1$ and $\alpha = \sqrt{5/6}(\beta = \sqrt{1/6})$. The solid and dashed lines denote the nondissipative case ($\Gamma = \kappa = 0$) and dissipative case ($\Gamma = G_0/30, \kappa = G_0/120$), respectively.

with a nonmonotonic curve accompanied by fast oscillation envelopes in the nondissipative case. This implies that during the dynamic evolution we can effectively control the QST and the fidelity can be maximized by only adjusting the peak amplitudes of Rabi frequencies of the laser. Specifically, the fidelities can reach 95% (91%) when Ω_0 is located in the regime of [0.03,0.49] ([0.02,0.22]) in the nondissipative (dissipative) case. Besides, as shown in Fig. 4(b), an approximately symmetrical curve represents the relationship between the fidelities and the detuning in both dissipative and nondissipative cases. In addition, we demonstrate numerically the QST performed with high fidelity for a very wide range of detuning. To obtain higher fidelity, the STIRAP process in our scheme can be optimized by elaborately adjusting the value of detuning Δ within the domains $[-0.12,-0.04]$ and [0.05,0.2] to try to keep fidelities beyond 95% in the nondissipative case. In contrast, the fidelities exceeding 90% in the dissipative case require the value of the detuning to be located in the region $[-0.15,0.25]$.

IV. DISCUSSION

We briefly address the experimental feasibility of our scheme. We employ the Zeeman levels $5S_{1/2}$ ($|F = 3\rangle$), $5S_{1/2}$ ($|F = 2\rangle$), and $5P_{3/2}$ ($|F = 3\rangle$) of the ^{85}Rb atom as the states $|g\rangle$, $|f\rangle$, and $|e\rangle$, respectively [30]. In our case, all time parameters are normalized in units of $1/G_0$, all frequency parameters are in units of G_0, and the waists (W_C and W_L) are in units of v/G_0. In addition, to meet the condition of global adiabaticity, we can choose the atomic velocity $v = 15$ m/s and atom-cavity interaction time $T_{in} \approx W_C/v = 120/G_0$ such that $G_0 T_{in} \gg 1$, $\Omega_0 T_{in} \gg 1$, and $\delta T_{in} \gg 1$ can be well satisfied. In contrast, our proposed realization demands a strong coupling cavity-QED system, so we choose the atomic and cavity decay rates as $\Gamma/2\pi \approx 5$ MHz and $\kappa/2\pi \approx 1.25$ MHz, respectively, and the atom-cavity coupling strength is $G_0/2\pi \approx 110$ MHz. Recently, an experimental group [31] has shown that the strong coupling regime $[g,\kappa,\Gamma]/2\pi = [10.6,1.3,3.0]$ MHz has been reached. Alternatively, a microcavity QED system [32–35], such as microtoroidal optical resonators with very small mode volumes, could offer much stronger coupling strengths reaching values in the *hundreds of* MHz, where the atoms are close to the surface of a microtoroid couple to the evanescent fields of whispering-gallery modes [32,33].

V. CONCLUSION

We have explored the atomic and cavity dissipation effects on the population dynamics in the STIRAP process. Based on the quantitative description of the noise effect in the STIRAP process, we have proposed theoretical research for realizing arbitrary QST between two traveling atoms in the cavity. By numerically simulating the Markovian master equation, we have shown that the fidelities of the QST can be maximized by elaborately adjusting the peak amplitudes of the laser's Rabi frequency and the detuning of the Raman transition. We have also shown that the system-environment interaction is unfavorable for increasing the fidelities of the QST. Our quantitative estimates of the robustness of the STIRAP process under lossy conditions would be useful for QIP exploration in atom-cavity QED systems.

ACKNOWLEDGMENTS

This work was supported by National Science Foundation of China under Grants No. 11074070, No. 11274351, No. 11274352, No. 11004226, No. 11004262, No. 10775176 and No. 10774163; the Aid Program for Science and Technology Innovative Research Team in Higher Educational Institute of Hunan Province; and the key Project of Science and Technology of Hunan Province under Grant No. 2010FJ2005.

APPENDIX: LINDBLAD EQUATION TRANSFORMATION METHOD

We describe below the transformation method for the Lindblad equation in details. In our case, the Hilbert space used is $9(N + 1)$ dimensions and the density matrix element has the form of $\rho_{ij,mn,kl}$, with $i,j,m,n = g$, e, or f and $k,l = 0,1,\ldots,N$, where we denote the states of atom 1 and atom 2 by i,m and j,n, respectively, and naturally k and l represent the number of photons in the cavity. Motivated by the simpler transformation method used for solving the master equation described in Refs. [7,27,28], we rearrange the $9(N + 1) \times 9(N + 1)$ elements of the density matrix ρ into a column vector $\vec{\rho}(t)$ of $[9(N + 1)]^2$ components. Thus the matrix differential equation (6) in the space of $9(N + 1) \times 9(N + 1)$ dimensions can be transformed to a vector differential equation in the Redfield space R of $[9(N + 1)]^2$ dimensions with general form as follows:

$$\frac{d}{dt}\vec{\rho}(t) = M\vec{\rho}(t), \tag{A1}$$

where M represents a matrix. The vector $\vec{\rho}(t)$ can be regarded as a summarization of the Bloch vector [27]

with the form $\vec{\rho}(t) = [\rho_{gg,gg,00}, \rho_{gg,gg,01}, \ldots, \rho_{gg,gg,NN}, \rho_{gg,ge,00}, \ldots, \rho_{gg,ge,NN}, \rho_{gg,gf,00}, \ldots, \rho_{gg,gf,NN}, \ldots, \rho_{ff,ff,00}, \ldots, \rho_{ff,ff,NN}]^T$, where the superscript T means the transpose of the vector.

A convenient basis $\{B_j\}$, $j = 1, \ldots, [9(N+1)]^2$, for a $9(N+1) \times 9(N+1)$ matrix should be introduced to simplify the following calculation. For example, it can be defined as

$$(B_j)_{kl} = \begin{cases} 1 & \text{under condition } C_1 \\ 0 & \text{otherwise,} \end{cases} \tag{A2}$$

where the condition C_1 is

$$\begin{aligned} 9(N+1)p < j \leqslant 9(N+1)(p+1), \\ k = p+1, \quad l = j - 9(N+1)p, \\ p \in \{0, 1, \ldots, 9N+8\}. \end{aligned} \tag{A3}$$

From Eqs. (A2) and (A3) we know that all the other elements of B_j are zero except one element with the value 1. Then, to ensure that the basis $\{B_j\}$ is orthonormal, one can define the scalar product of two random operators $\hat{U}$ and $\hat{V}$ in R as $(\hat{U}, \hat{V}) = \mathrm{Tr}(\hat{U}^\dagger \hat{V})$. Therefore, any operator $\hat{U}$ produced in R can be represented by the coefficient u_j,

$$\hat{U} = \sum_{j=1}^{[9(N+1)]^2} u_j B_j, \tag{A4}$$

with the coefficient $u_j = \mathrm{Tr}(B_j^\dagger \hat{U})$.

It is noticeable that the master equation (6) has three different terms with the forms $U\rho$, ρV, and $U\rho V$. We replace it with the matrix forms for products of the operators $\hat{U}\hat{\rho}$, $\hat{\rho}\hat{V}$, and $\hat{U}\hat{\rho}\hat{V}$, respectively, in R. Thus we also can define the operator products $\hat{U}\hat{\rho}$ with the same form of $\hat{U}$ in Eq. (A4) as

$$\hat{U}\hat{\rho} = \sum_{j=1}^{[9(N+1)]^2} (\hat{U}\hat{\rho})_j B_j. \tag{A5}$$

Then the coefficient $(\hat{U}\hat{\rho})_j$ can be derived from Eq. (A5) with the form

$$\begin{aligned} (\hat{U}\hat{\rho})_j = \mathrm{Tr}(B_j^\dagger \hat{U}\hat{\rho}) &= \sum_{l=1}^{[9(N+1)]^2} \sum_{k=1}^{[9(N+1)]^2} u_l \rho_k \mathrm{Tr}(B_j^\dagger B_l B_k) \\ &= \sum_{k=1}^{[9(N+1)]^2} (M_U)_{jk} \rho_k, \end{aligned} \tag{A6}$$

where we have set

$$(M_U)_{jk} = \sum_{l=1}^{[9(N+1)]^2} u_l \mathrm{Tr}(B_j^\dagger B_l B_k). \tag{A7}$$

Therefore, we can transform Eq. (A6) into reduced general vector forms $\overrightarrow{U\rho} = M_U \vec{\rho}$.

We also can obtain $\overrightarrow{\rho V} = M_V \vec{\rho}$ corresponding to

$$(M_V)_{jk} = \sum_{l=1}^{[9(N+1)]^2} v_l \mathrm{Tr}(B_j^\dagger B_k B_l)$$

and $\overrightarrow{\rho V} = M_V \vec{\rho}$ together with

$$(M_{UV})_{jk} = \sum_{l,s=1}^{[9(N+1)]^2} u_l v_s \mathrm{Tr}(B_j^\dagger B_l B_k B_s)$$

using the same procedure of Eqs. (A5)–(A7). As a result, we have transformed $\hat{U}\hat{\rho}$, $\hat{\rho}\hat{V}$, and $\hat{U}\hat{\rho}\hat{V}$ into $M_U\vec{\rho}(t)$, $M_V\vec{\rho}(t)$, and $M_{UV}\vec{\rho}(t)$ in the space R, respectively.

[1] K. Bergmann, H. Theuer, and B. W. Shore, Rev. Mod. Phys. **70**, 1003 (1998).

[2] N. V. Vitanov, M. Fleischhauer, B. W. Shore, and K. Bergmann, in *Advances in Atomic, Molecular, and Optical Physics*, edited by H. Walther and B. Bederson, Vol. 46 (Academic, New York, 2001), pp. 55–190.

[3] N. Vitanov, T. Halfmann, B. Shore, and K. Bergmann, Annu. Rev. Phys. Chem. **52**, 763 (2001).

[4] R. Unanyan, M. Fleischhauer, B. W. Shore, and K. Bergmann, Opt. Commun. **155**, 144 (1998).

[5] H. R. Gray, R. M. Whitley, and C. R. Stroud, Opt. Lett. **3**, 218 (1978).

[6] J.-Y. Gao, C. Guo, X.-Z. Guo, G.-X. Jin, Q.-W. Wang, J. Zhao, H.-Z. Zhang, Y. Jiang, D.-Z. Wang, and D.-M. Jiang, Opt. Commun. **93**, 323 (1992).

[7] H. Eleuch, S. Guérin, and H. R. Jauslin, Phys. Rev. A **85**, 013830 (2012).

[8] I. I. Boradjiev and N. V. Vitanov, Phys. Rev. A **82**, 043407 (2010).

[9] D. Yan, C.-L. Cui, M. Zhang, and J.-H. Wu, Phys. Rev. A **84**, 043405 (2011).

[10] M. Sukharev and S. A. Malinovskaya, Phys. Rev. A **86**, 043406 (2012).

[11] B. Rousseaux, S. Guérin, and N. V. Vitanov, Phys. Rev. A **87**, 032328 (2013).

[12] D. Petrosyan, and K. Mølmer, Phys. Rev. A **87**, 033416 (2013).

[13] V. S. Malinovsky and J. L. Krause, Eur. Phys. J. D **14**, 147 (2001).

[14] M. Glässl, A. M. Barth, K. Gawarecki, P. Machnikowski, M. D. Croitoru, S. Lüker, D. E. Reiter, T. Kuhn, and V. M. Axt, Phys. Rev. B **87**, 085303 (2013).

[15] H. Maeda, J. H. Gurian, and T. F. Gallagher, Phys. Rev. A **83**, 033416 (2011).

[16] R. T. Brierley, C. Creatore, P. B. Littlewood, and P. R. Eastham, Phys. Rev. Lett. **109**, 043002 (2012).

[17] J. S. Melinger, S. R. Gandhi, A. Hariharan, J. X. Tull, and W. S. Warren, Phys. Rev. Lett. **68**, 2000 (1992).

[18] B. Y. Chang, I. R. Sola, V. S. Malinovsky, and J. Santamaria, Phys. Rev. A **64**, 033420 (2001).

[19] X. H. Yang, Z. R. Sun, and Z. G. Wang, Phys. Rev. A **76**, 043417 (2007).

[20] L. P. Yatsenko, B. W. Shore, T. Halfmann, K. Bergmann, and A. Vardi, Phys. Rev. A **60**, R4237 (1999); A. A. Rangelov, N. V. Vitanov, L. P. Yatsenko, B. W. Shore, T. Halfmann, and K. Bergmann, *ibid.* **72**, 053403 (2005); M. Oberst, H. Münch, and T. Halfmann, Phys. Rev. Lett. **99**, 173001 (2007).

[21] L. F. Wei, J. R. Johansson, L. X. Cen, S. Ashhab, and F. Nori, Phys. Rev. Lett. **100**, 113601 (2008).

[22] J.-H. Schönfeldt, J. Twamley, and S. Rebić, Phys. Rev. A **80**, 043401 (2009).

[23] E. A. Shapiro, V. Milner, C. Menzel-Jones, and M. Shapiro, Phys. Rev. Lett. **99**, 033002 (2007).

[24] S. Zhdanovich, E. A. Shapiro, J. W. Hepburn, M. Shapiro, and V. Milner, Phys. Rev. A **80**, 063405 (2009).

[25] M. Amniat-Talab, S. Lagrange, S. Guerin, and H. R. Jauslin, Phys. Rev. A **70**, 013807 (2004).

[26] M. Scala, B. Militello, A. Messina, and N. V. Vitanov, Phys. Rev. A **81**, 053847 (2010); **83**, 012101 (2011).

[27] S. G. Schirmer, T. Zhang, and J. V. Leahy, J. Phys. A **37**, 1389 (2004).

[28] A. I. Solomon and S. G. Schirmer, in *Group 24: Physical and Mathematical Aspects of Symmetry*, IOP Conf. Proc. No. 173 (Institute of Physics, London, 2003), p. 485.

[29] M. A. Nielsen and I. L. Chuang, *Quantum Computation and Quantum Information* (Cambridge University Press, Cambridge, 2000).

[30] M. Hennrich, T. Legero, A. Kuhn, and G. Rempe, Phys. Rev. Lett. **85**, 4872 (2000).

[31] F. Brennecke, T. Donner, S. Ritter, T. Bourdel, U. Köhl, and T. Esslinger, Nature (London) **450**, 268 (2007).

[32] T. Aoki, B. Dayan, E. Wilcut, W. P. Bowen, A. S. Parkins, T. J. Kippenberg, K. J. Vahala, and H. J. Kimble, Nature (London) **443**, 671 (2006).

[33] B. Dayan, A. S. Parkins, T. Aoki, H. J. Kimble, E. P. Ostby, and K. J. Vahala, Science **319**, 1062 (2008).

[34] C. Junge, D. O'shea, J. Volz, and A. Rauschenbeutel, Phys. Rev. Lett. **110**, 213604 (2013).

[35] A. L. Grimsmo and S. Parkins, Phys. Rev. A **87**, 033814 (2013).